Hye-Jin Lee,[1] Shin-Bum Jo,[1] Anthony I. Romer,[2,3] Hyo-Jeong Lim,[1] Min-Jung Kim,[4] Seung-Hoi Koo,[4] Robert S. Krauss,[2,3] and Jong-Sun Kang[1]

Overweight in Mice and Enhanced Adipogenesis In Vitro Are Associated With Lack of the Hedgehog Coreceptor Boc

Diabetes 2015;64:2092–2103 | DOI: 10.2337/db14-1017

OBESITY STUDIES

Obesity arises from a combination of genetic, environmental, and behavioral factors. However, the processes that regulate white adipose tissue (WAT) expansion at the level of the adipocyte are not well understood. The Hedgehog (HH) pathway plays a conserved role in adipogenesis, inhibiting fat formation in vivo and in vitro, but it has not been shown that mice with reduced HH pathway activity have enhanced adiposity. We report that mice lacking the HH coreceptor BOC displayed age-related overweight and excess WAT. They also displayed alterations in some metabolic parameters but normal food intake. Furthermore, they had an exacerbated response to a high-fat diet, including enhanced weight gain and adipocyte hypertrophy, livers with greater fat accumulation, and elevated expression of genes related to adipogenesis, lipid metabolism, and adipokine production. Cultured *Boc*$^{-/-}$ mouse embryo fibroblasts showed enhanced adipogenesis relative to *Boc*$^{+/+}$ cells, and they expressed reduced levels of HH pathway target genes. Therefore, a loss-of-function mutation in an HH pathway component is associated with WAT accumulation and overweight in mice. Variant alleles of such HH regulators may contribute to WAT accumulation in human individuals with additional genetic or lifestyle-based predisposition to obesity.

The prevalence of obesity and associated metabolic pathologies has attracted attention to the identification of etiological factors (1,2). Obesity arises from genetic, environmental, and behavioral factors that influence energy balance. The principal feature of obesity is excessive accumulation of white adipose tissue (WAT) (1,3–5). Although obesity is understood to be a centrally regulated consequence of overnutrition and/or reduced expenditure of energy, the processes that regulate WAT expansion at the level of the adipocyte are not well characterized.

WAT expansion occurs through adipocyte hypertrophy and hyperplasia, so such processes presumably engage at some level the process of adipogenesis (3,4). Adipogenesis has been analyzed with preadipocyte cell lines such as 3T3-L1 and various mutant mouse lines (6). These studies elucidated a transcriptional network centered around PPARγ and C/EBP family members, which drive differentiation of preadipocytes into lipid-accumulating adipocytes (6). Recent studies have identified cells in the stromal vascular fraction (SVF) of WAT that are bona fide adipocyte progenitor cells (7,8). Such cells in WAT must respond to hormonal and local cues that regulate homeostatic maintenance of this tissue. The cues that act on adipocyte progenitor cells are not well understood, but among those implicated is the Hedgehog (HH) signaling pathway.

HH proteins regulate developmental events in organisms as diverse as insects and mammals. Among mammalian HH proteins, Sonic Hedgehog (SHH) plays the broadest role and is involved in the growth and/or morphogenesis of many body structures (9). HH proteins activate a conserved signal transduction pathway (10–12).

[1]Department of Molecular Cell Biology, Sungkyunkwan University School of Medicine, Samsung Biomedical Research Institute, Suwon, Republic of Korea
[2]Department of Developmental and Regenerative Biology, Icahn School of Medicine at Mount Sinai, New York, NY
[3]Graduate School of Biological Sciences, Icahn School of Medicine at Mount Sinai, New York, NY
[4]Division of Life Sciences, Korea University, Seoul, Republic of Korea

Corresponding authors: Jong-Sun Kang, kangj01@skku.edu, and Robert S. Krauss, robert.krauss@mssm.edu.

Received 1 July 2014 and accepted 1 January 2015.

H.-J.L. and S.-B.J. contributed equally to this work.

In the absence of ligand, the primary HH receptor PTCH1 functions to inhibit signaling by a second membrane protein, SMO. Binding of HH to PTCH1 relieves inhibition of SMO, and SMO signals to activate pathway target genes via GLI transcription factors. Among such target genes are *Gli1* and *Ptch1* themselves, and they are often used as readouts of pathway activity (10–12).

CDO (also called CDON), BOC, and GAS1 are cell surface proteins that promote HH pathway activity as ligand-binding coreceptors with PTCH1 (13–20). CDO and BOC are related transmembrane proteins (21,22), whereas GAS1 is a GPI-anchored protein unrelated to CDO and BOC (23). Analysis of mice with targeted mutations in *Cdon*, *Boc*, and *Gas1* revealed that although none is essential for HH pathway activity, they are collectively required for pathway function in the early mouse embryo (13,14,16,19). A ternary complex of HH ligand, PTCH1, and at least one of these coreceptors appears to be required for successful signal transduction (15,16,24). *Boc*-null mice, the subject of this study, are viable and fertile but display defects in SHH-dependent neural patterning and axon guidance (19,25–28).

The HH pathway negatively regulates adipogenesis. Activation of the HH pathway with either SHH or the SMO agonist purmorphamine inhibited adipogenesis of 3T3-L1 and additional cell lines (29–32). Furthermore, blockade of HH signaling, with a dominant-negativeform of GLI2 or the SMO antagonist cyclopamine, enhanced adipogenesis of these cells in response to inducing factors (31,32). HH signals blocked early steps of adipogenesis, upstream of the expression of PPARγ (29,31,32). These studies suggest that the HH pathway functions to block differentiation of preadipocytes in vitro. Experiments in mice are consistent with this notion. Adult mice homozygous for a hypomorphic allele of *Ptch1* showed reduced WAT mass, which had lower levels of adipose markers and elevated levels of HH target genes (33). Adipose tissue–specific mutation of another HH pathway inhibitor, *Sufu*, led to a loss of WAT (34). Finally, mice with diet-induced or genetic (*ob*/*ob*) obesity displayed decreased expression of HH pathway components (31).

Although mice with a genetic gain of function in HH pathway activity showed loss of WAT (33,34), it has not been demonstrated that mice with a loss of HH activity have enhanced adiposity. We report that mice with a germline mutation in *Boc* display age-dependent overweight due to an increase in WAT. These mice also show an exaggerated response to a high-fat diet (HFD), and $Boc^{-/-}$ embryo fibroblasts differentiate into adipocytes more efficiently than wild-type cells. These results reveal that BOC, presumably acting as an SHH coreceptor, is required for maintenance of normal weight in vivo and appropriate regulation of adipogenic differentiation in vitro.

RESEARCH DESIGN AND METHODS

Mice

$Boc^{AP\text{-}1}$ mice (19) were backcrossed onto a C57BL/6N background for at least six generations. For age-related effects, male $Boc^{+/+}$ or $Boc^{-/-}$ mice backcrossed for six generations were used and weighed every 4 weeks over 32 weeks. To assess food intake, food was weighed and replenished every other day for individually caged mice for 2 weeks. For HFD-induced effects, male $Boc^{+/+}$ or $Boc^{-/-}$ mice backcrossed for 10 generations were used. Four-week-old mice were fed with HFD (60% fat content; Harlan) and weighed weekly over 8 weeks. For blood glucose levels, tail vein blood was used after animals were fasted for 16 h, with free access to water. For the glucose tolerance test (GTT), mice were fasted for 16 h and injected intraperitoneally with 1.5 g 20% D-glucose/kg body weight (Sigma-Aldrich), followed by measurement of blood glucose levels. For the insulin tolerance test (ITT), mice were fasted for 6 h and injected intraperitoneally with 1 IU insulin/kg body weight (Sigma-Aldrich), followed by measurement of glucose levels. Mouse tissues were immediately frozen in liquid nitrogen and stored at −70°C or fixed in 4% paraformaldehyde (PFA). Plasma insulin was measured with the Mouse Insulin ELISA Kit (U-type; Shibayagi Corp.), and serum triglycerides and nonesterified fatty acids were measured by colorimetric assay kits (Wako).

For assessment of metabolic parameters (Fig. 2), 5-month-old $Boc^{+/+}$ and $Boc^{-/-}$ mice were analyzed with metabolic cages (Harvard Apparatus; Panlab). Measurements were performed for 48 h, during which animals had access to food and water. Core body temperature was measured with an HB-101 homeothermic blanket/pad equipment (Harvard Apparatus).

Histology, Oil Red O Staining, and Placental Alkaline Phosphatase Staining

For hematoxylin-eosin (H-E) staining, WAT and liver tissues were fixed and processed for 20-μm paraffin sections. For Oil Red O staining, livers were fixed in 4% PFA and dehydrated by sucrose gradient followed by an optimal cutting temperature compound-cryosection (10 μm) and Oil Red O staining. For Oil Red O staining of differentiated mouse embryonic fibroblasts (MEFs) and 3T3-L1 cells, cultures were fixed in 10% formaldehyde for 10 min and stained with Oil Red O. Stained plates were treated with 1 mL isopropanol/4% NP-40 for 10 min by a gentle shaking, and extracted Oil Red O was quantified by measuring optical density at 520 nm. For placental alkaline phosphatase (PLAP) staining, tissues were fixed with 2% PFA plus 0.2% glutaraldehyde for 2 h at 4°C, washed in PBS, permeabilized in 0.3% Triton overnight at 4°C, washed in saline, heat inactivated for 30 min at 72°C, washed in NTM (100 mmol/L NaCl, 100 mmol/L Tris-HCl, pH 9.5, 50 mmol/L $MgCl_2$) buffer, and stained with BM purple (Roche).

Cell Cultures

Preparation of the SVF from WAT was performed as previously described (8). In brief, WAT was minced with

scissors and digested with 2 mg/mL Collagenase I (Sigma-Aldrich) in DMEM at 37°C for 1 h. DMEM plus 10% FBS was added to double the volume, floating adipocytes were removed, and the digest was filtered through a 100-μm mesh that retained vessels of the stromal-particulate fraction. The filtrate was centrifuged at 800*g* for 5 min, and the SVF pellet was resuspended in DMEM containing 10% FBS and cultured for 2 days.

Isolation of primary MEFs was carried out as previously described (35). 3T3-L1 cells and MEFs were cultured in growth medium (DMEM plus 10% FBS) at subconfluence. For adipocyte differentiation, cells were grown to confluence and switched into differentiation medium I (growth medium plus 0.5 μmol/L IBMX, 1 μg/μL insulin, 0.25 μmol/L dexamethazone, 2 μmol/L rosiglitazone; Sigma-Aldrich) for 2 days. The culture medium was then changed to differentiation medium II (growth medium plus 2 μmol/L rosiglitazone), and the medium was changed every 2 days. To activate SHH signaling, MEFs were treated with 250 ng/mL SHH (R&D Systems) or 5.2 μmol/L purmorphamine (Calbiochem) in differentiation media from differentiation day 2 onward.

Immunoblotting

Immunoblotting was performed as previously described (15). Antibodies used are listed in Table 1.

PCR and Quantitative RT-PCR Analysis

Tissues were homogenized with FastPrep-24 (MP Biomedicals) and extracted with the RNA Extraction Kit (iNtRON). cDNA was generated with PrimeScript RT Reagent Kit (Takara) and amplified with *n*Taq polymerase (Enzynomics). Quantitative RT-PCR (qRT-PCR) was performed with SYBR Green (Takara) and analyzed with a TP8000 System (Takara). All data are normalized to the expression of ribosomal protein–encoding *L32*. Primers used in this study are listed in Table 2.

Table 1—The antibodies used in this study

CDO	R&D Systems
BOC	R&D Systems
Gli1	Santa Cruz Biotechnology
Gas1	Santa Cruz Biotechnology
Ptch1	Santa Cruz Biotechnology
C/EBPα	Santa Cruz Biotechnology
FAS	Abcam
PPARγ	Santa Cruz Biotechnology
SCD1	Santa Cruz Biotechnology
Acc	Cell Signaling Technology
aP2	Cayman
SREBP1c	Santa Cruz Biotechnology
β-Actin	Sigma-Aldrich
HSP90	Santa Cruz Biotechnology

Table 2—The primer sequences used in this study

Boc	Forward	5′AGCAGCTGGTGAGTTGAGTC3′
	Backward	5′GGAGCTTGCCCAGCAGC3′
Cdo	Forward	5′GCAACCAGAAAGGGAAGGGT3′
	Backward	5′GAGCTCAGACTTGGCACCTT3′
Ptch1	Forward	5′GCCACAGCCCCTAACAAAA3′
	Backward	5′CCCACAATCAACTCCTCCTG3′
Gli1	Forward	5′TCGACCTGCAAACCGTAATCC3′
	Backward	5′TCCTAAAGAAGGGCTCATGGTA3′
Gas1	Forward	5′GGAACACTG ACCCACACTCT3′
	Backward	5′AAAGACCCCCACCGTTCAG3′
Ccl5	Forward	5′TGCCCACGTCAAGGAGTATTT3′
	Backward	5′TTCTCTGGGTTGGCACACACT3′
Cebpα	Forward	5′GAACAGCAACGAGTACCGGGT3′
	Backward	5′CCATGGCCTTGACCAAGGAG3′
Fas1	Forward	5′GCTGCGGAAACTTCAGGAAAT3′
	Backward	5′AGAGACGTGTCACTCCTGGACTT3′
Pparα	Forward	5′AGGGTTGAGCTCAGTCAGGA3′
	Backward	5′GGTCACCTACGAGTGGCATT3′
Pparγ	Forward	5′TTCAGAAGTGCCTTGCTGTG3′
	Backward	5′GCTGGTCGATATCACTGGAGA3′
Scd1	Forward	5′CCGGGCCCCTTAGATCGA3′
	Backward	5′TAGCCTGTAAAAGATTTCTGCA3′
Acc	Forward	5′CGCGGAGGAGTTCCTAATTC3′
	Backward	5′TGTCCCAGACGTAAGCCTTC3′
aP2	Forward	5′AAGGTGAAGAGCATCATAACCCT3′
	Backward	5′TCACGCCTTTCATAACACATTCC3′
TNFα	Forward	5′AGCCCCCAGTCTGTATCCTT3′
	Backward	5′CTCCCTTTGCAGAACTCAGG3′
β-Actin	Forward	5′GTCCCTGACCCTCCCAAAAG3′
	Backward	5′GCTGCCTCAACACCTCAACCC3′
Ucp1	Forward	5′TGCCCACGTCAAGGAGTATTT3′
	Backward	5′TTCTCTGGGTTGGCACACT
Ucp2	Forward	5′ACTGTCGAAGCCTACAAGAC3′
	Backward	5′CACCAGCTCAGTACAGTTGA3′
Ucp3	Forward	5′GCCTGTGGAAAGGGACTTGG3′
	Backward	5′GGAGCGTTCATGTATCGGGT3′

Imaging

Microscopy was performed on a Nikon ECLIPSE TE2000-U with NIS-Elements F software (Nikon), Zeiss AxioPlan 2, and Zeiss AxioPlan 2 IE microscopes. Adipocytes were traced and their area measured using ImageJ software.

Statistical Analysis

Values are means ± SEM or SD as noted. Statistical significance was calculated by paired or unpaired two-tailed Student *t* test; differences were considered significant at $P < 0.05$.

RESULTS

Age-Related Overweight in Mice Lacking BOC

Body weights of $Boc^{+/+}$ and $Boc^{-/-}$ mice fed normal chow were measured on a monthly basis from 4 to 32 weeks of age. $Boc^{-/-}$ mice were significantly heavier than $Boc^{+/+}$ mice by 16 weeks of age and weighed 16% more than control animals at 32 weeks of age (Fig. 1*A*). Therefore,

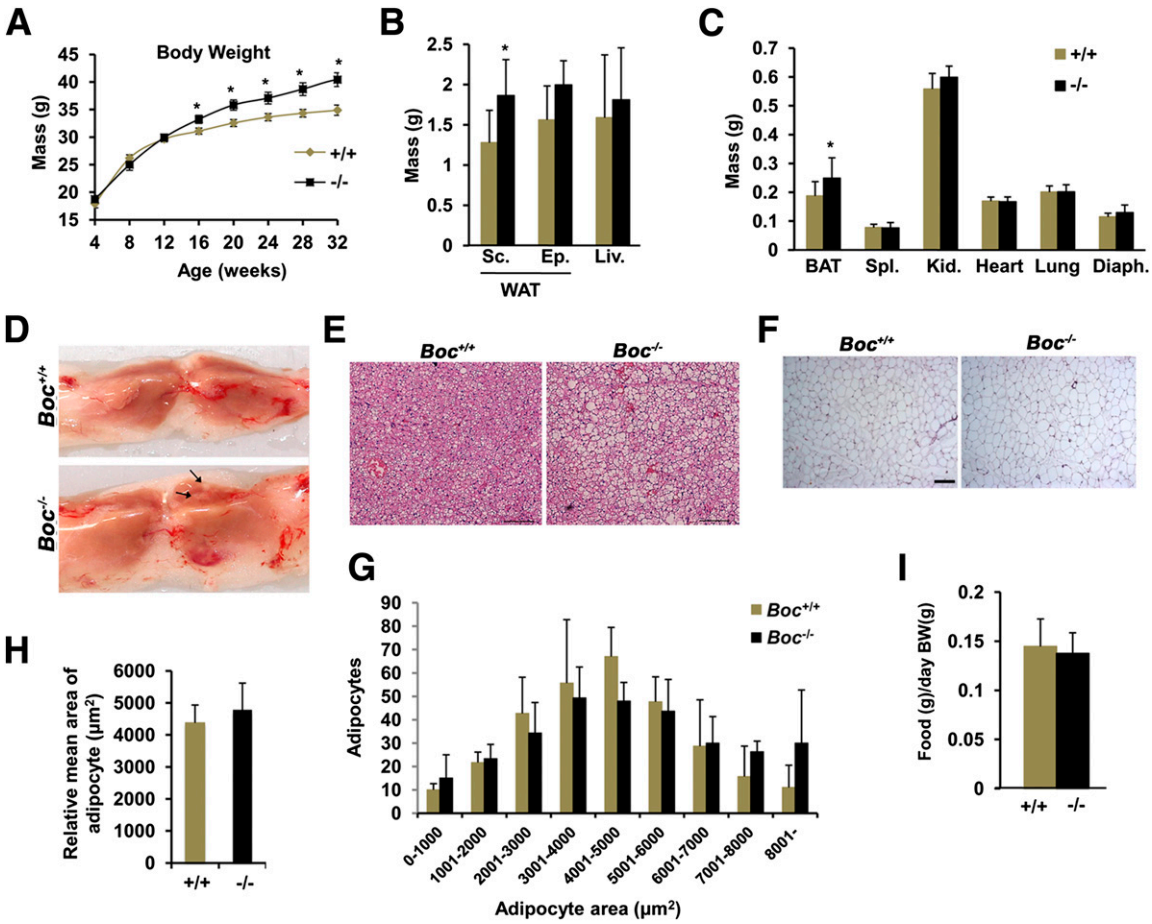

Figure 1—Age-related overweight in $Boc^{-/-}$ mice. *A*: Time course of body weight in $Boc^{+/+}$ (+/+) and $Boc^{-/-}$ (−/−) mice. Values are means ± SEM; n = 31–42 for $Boc^{+/+}$ mice and n = 25–43 for $Boc^{-/-}$ mice at various time points. *$P < 0.01$. *B* and *C*: Weights of individual organs or tissues dissected from +/+ and −/− mice. Diaph., diaphragm; Ep., epididymal WAT; Kid., kidney; Liv., liver; Sc., subcutaneous WAT; Spl., spleen. Values are means ± SD; n = 12–14 for each tissue. *$P < 0.05$. *D*: Dissected BAT from $Boc^{+/+}$ and $Boc^{-/-}$ mice. Note that the $Boc^{-/-}$ BAT is paler than that of the control and has areas of obvious whitening (arrows). *E*: H-E–stained sections of BAT from $Boc^{+/+}$ and $Boc^{-/-}$ mice. Bar, 50 μm. *F*: H-E–stained sections of WAT from $Boc^{+/+}$ and $Boc^{-/-}$ mice. Bar, 50 μm. *G*: Average area of adipocytes from sections of adult WAT from +/+ and −/− mice. Values are means ± SD; n = 3. *H*: Distribution of adipocyte areas from sections of adult WAT from +/+ and −/− mice. Values are means ± SD; n = 3. *I*: Food intake by 24-week-old +/+ and −/− mice. BW, body weight. Values are means ± SD; n = 7.

BOC-deficient mice displayed age-dependent overweight. To determine whether this phenotype was due to increased adiposity, the weight of WAT and other tissues from 32-week-old $Boc^{+/+}$ and $Boc^{-/-}$ mice was analyzed. $Boc^{-/-}$ mice had significantly more subcutaneous WAT than $Boc^{+/+}$ mice; mutants also had somewhat more epididymal (visceral) WAT, although this was not statistically significant (Fig. 1*B*). Weights of other tissues, including liver, spleen, kidney, heart, lungs, and diaphragm, were not different from those of $Boc^{+/+}$ mice (Fig. 1*B* and *C*). $Boc^{-/-}$ mice exhibited a greater amount of brown adipose tissue (BAT) (Fig. 1*C*), which had a pale appearance with areas of obvious whitening (Fig. 1*D*) and enlarged lipid droplets (Fig. 1*E*). The mean area of WAT adipocytes was similar between $Boc^{+/+}$ and $Boc^{-/-}$ mice; the mutants had more adipocytes of the largest size, but this difference was not statistically significant (Fig. 1*F–H*). Finally, $Boc^{+/+}$ and $Boc^{-/-}$ animals consumed similar amounts of food per day (Fig. 1*I*). These data suggest that BOC-deficient mice became overweight from a modest but progressive increase in adiposity.

Since $Boc^{-/-}$ mice were not hyperphagic, we assessed whether decreased energy expenditure contributed to their increased adiposity. Normal chow-fed 5-month-old $Boc^{+/+}$ and $Boc^{-/-}$ mice (Fig. 2*A*) were used to assess whole-body metabolic rate. $Boc^{-/-}$ mice exhibited slightly lower body temperature than $Boc^{+/+}$ mice (Fig. 2*B*). Spontaneous locomotive activity in $Boc^{-/-}$ mice averaged about half that in control mice but this difference was not statistically significant, and there was no difference in rearing activity (Fig. 2*C* and *D*). $Boc^{-/-}$ mice exhibited slightly decreased oxygen consumption and carbon dioxide production during the light phase (Fig. 2*E* and *F*). Respiratory quotient was slightly lower in $Boc^{-/-}$ mice in both dark and light phases but was within normal range (Fig. 2*G*). Energy expenditure by $Boc^{-/-}$ mice was

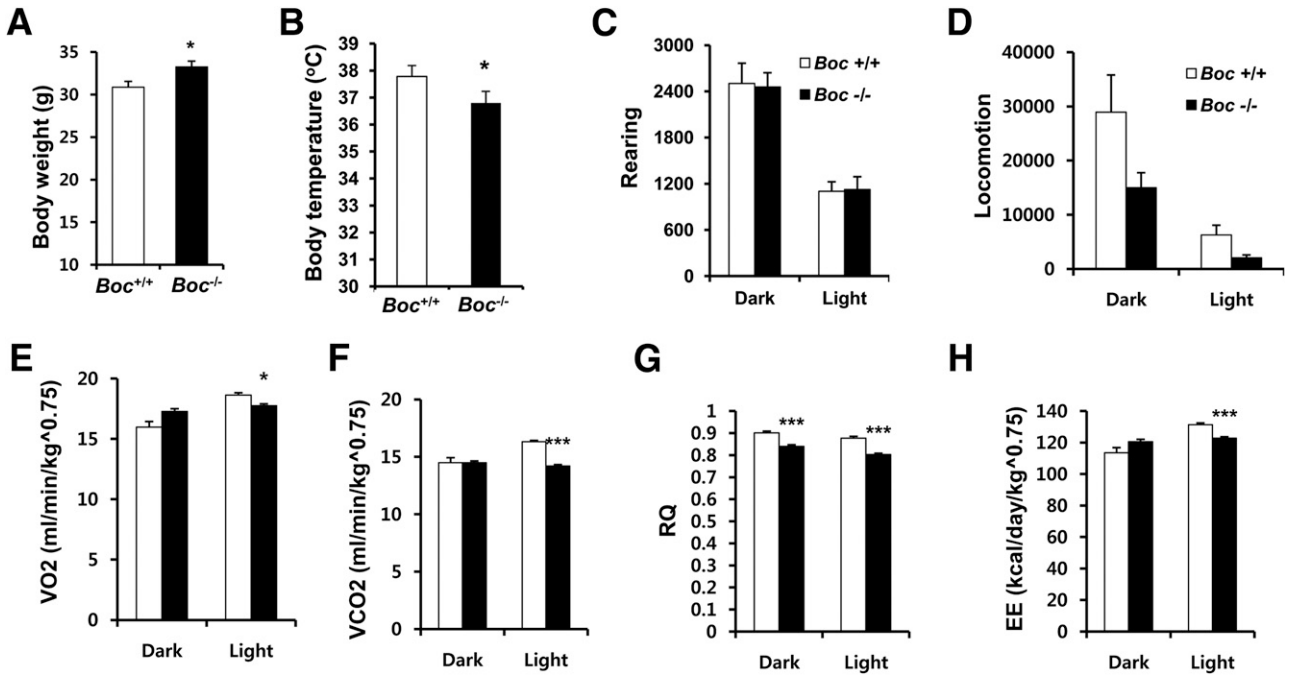

Figure 2—Alterations in whole-body metabolism of $Boc^{-/-}$ mice. *A*: Body weights. *B*: Body temperature. *C*: Rearing activity. *D*: Locomotion. *E*: O_2 consumption (VO2). *F*: CO_2 production (VCO2). *G*: Respiratory quotient (RQ). *H*: Energy expenditure (EE). Normal chow-fed, 5-month-old $Boc^{+/+}$ and $Boc^{-/-}$ mice were measured with metabolic cages (n = 6). Data in *A–H* represent means ± SEM. ***$P < 0.001$; *$P < 0.05$.

also slightly decreased during the light phase (Fig. 2*H*), but total energy expenditure (dark plus light) was not different. These results suggest $Boc^{-/-}$ mice have alterations of whole-body metabolism that may contribute to their overweight.

Exacerbated Response to HFD by BOC-Deficient Mice

As BOC deficiency predisposed mice to greater adiposity, we challenged 6-week-old mice with HFD for a total of 8 weeks. Beginning at the third week, $Boc^{-/-}$ mice gained more body weight than $Boc^{+/+}$ mice under both diets, but the difference between mutant and control mice was greater on HFD than normal chow (Fig. 3*A* and *B*). To determine whether enhanced weight gain in $Boc^{-/-}$ mice was accompanied by abnormal glucose homeostasis, we measured steady-state blood glucose levels and performed tolerance tests for glucose and insulin after 7 weeks of HFD. Prior to challenge, blood glucose levels were similar between control and mutant mice (Fig. 3*C*). Under glucose challenge, a spike in blood glucose levels was observed at 15 min, followed by a slower further increase and progressive return to near baseline in both $Boc^{+/+}$ and $Boc^{-/-}$ mice. However, $Boc^{-/-}$ mice had higher blood glucose levels at the 15- and 30-min time points than $Boc^{+/+}$ mice (Fig. 3*D*). In the ITT, prior to insulin injection, $Boc^{-/-}$ mice had slightly, but not statistically significantly, lower blood insulin levels than $Boc^{+/+}$ mice (Fig. 3*F*). Serum glucose levels decreased sharply 15–45 min after insulin injection in both $Boc^{+/+}$ and $Boc^{-/-}$ mice, but $Boc^{-/-}$ mice displayed significantly less sensitivity to insulin (Fig. 3*E*). Therefore, $Boc^{-/-}$ mice on HFD had perturbations in glucose homeostasis. Furthermore, when on HFD, mutant animals also showed elevated plasma levels of triglycerides and nonesterified fatty acids as compared with $Boc^{+/+}$ mice (Fig. 3*G* and *H*).

We next assessed livers and WAT of $Boc^{+/+}$ and $Boc^{-/-}$ mice after 8 weeks of HFD. $Boc^{-/-}$ livers displayed more and larger lipid droplets than $Boc^{+/+}$ livers upon Oil Red O staining (Fig. 4*A*). Hepatic lipid accumulation is often associated with enhanced expression of genes involved in lipid metabolism (e.g., *Acc*, *Fas*, *Scd1*, and *aP2*) and that promote adipogenesis (e.g., *Pgc1α*, *Cebpα*, *Srebp1c*, and *Pparγ*) (6). We therefore assessed by qRT-PCR and Western blot analyses the expression of these genes in livers of $Boc^{+/+}$ and $Boc^{-/-}$ mice on HFD. Expression of all these genes was enhanced in $Boc^{-/-}$ livers relative to controls (Fig. 4*C–E*). H-E staining of WAT revealed that adipocytes from $Boc^{-/-}$ mice on HFD were larger than those of $Boc^{+/+}$ mice on this diet (Fig. 4*A* and *B*). We then assessed the expression of lipid metabolism, adipogenic, and adipokine-encoding genes (*Ccl5* and *TNFα*) in WAT from $Boc^{+/+}$ and $Boc^{-/-}$ mice on HFD. Expression of all these genes was significantly higher in $Boc^{-/-}$ WAT than $Boc^{+/+}$ WAT (Fig. 4*F* and *G*). Finally, expression of uncoupling protein (*Ucp*) 1, 2, and 3 genes was assessed by qRT-PCR in BAT. *Ucp1* and *Ucp3* expression was significantly reduced in $Boc^{-/-}$ BAT (Fig. 4*H*). Taken together, it is concluded that $Boc^{-/-}$ mice showed an exaggerated response when challenged with HFD.

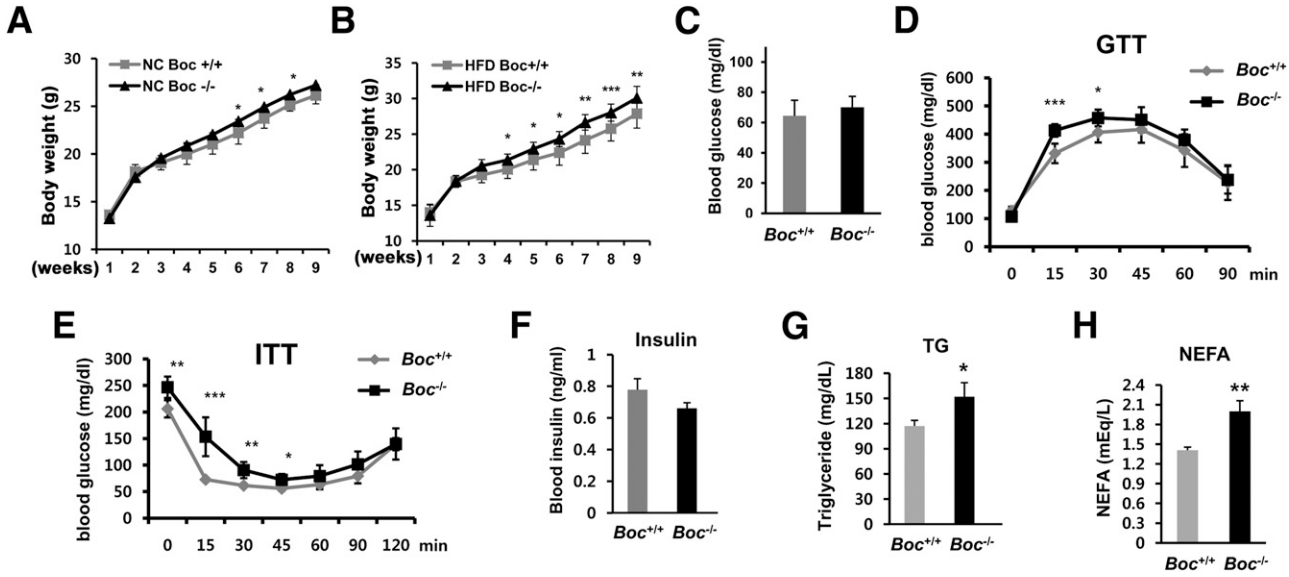

Figure 3—Exacerbated responses to HFD by $Boc^{-/-}$ mice. Time course of body weight in $Boc^{+/+}$ and $Boc^{-/-}$ mice on normal chow (NC) (*A*) and HFD (*B*). Values are means ± SEM; n = 5–7 for each time point. $^{*}P < 0.05$; $^{**}P < 0.005$; $^{***}P < 0.001$. *C*: Blood glucose levels in $Boc^{+/+}$ and $Boc^{-/-}$ mice on HFD for 8 weeks and then fasted for 16 h. *D*: GTT in $Boc^{+/+}$ and $Boc^{-/-}$ mice on HFD for 8 weeks and then fasted for 16 h. Mice were administered glucose intraperitoneally, and blood glucose levels were measured every 15 min for 2 h. Values are means ± SEM; n = 5–7. $^{***}P < 0.01$; $^{*}P < 0.5$. *E*: ITT in $Boc^{+/+}$ and $Boc^{-/-}$ mice on HFD for 8 weeks and then fasted for 6 h. Mice were administered insulin intraperitoneally, and blood glucose levels were measured every 15 min for 2 h. Values are means ± SEM; n = 5–7. $^{***}P < 0.001$; $^{**}P < 0.005$; $^{*}P < 0.05$. *F*: Plasma insulin levels in $Boc^{+/+}$ and $Boc^{-/-}$ mice on HFD for 8 weeks. *G*: Serum triglyceride (TG) levels in $Boc^{+/+}$ and $Boc^{-/-}$ mice on HFD for 8 weeks. $^{*}P < 0.05$. *H*: Blood nonesterified fatty acid (NEFA) levels in $Boc^{+/+}$ and $Boc^{-/-}$ mice on HFD for 8 weeks. $^{**}P < 0.005$.

Enhanced Adipogenesis in $Boc^{-/-}$ MEFs

To gain information on potential sites of action relevant to the phenotypes of overweight and HFD response, *Boc* expression was examined in adult tissues by qRT-PCR. Highest levels of *Boc* expression were seen in brain, lung, and WAT; expression in liver was barely detectable (Fig. 5*A*). The mutant *Boc* allele contains a PLAP reporter gene, which faithfully reflects endogenous *Boc* expression (19,36). The PLAP reporter was expressed at high levels in WAT from $Boc^{+/PLAP}$ mice (Fig. 5*B*). To investigate which cell types in WAT express *Boc*, mature adipocytes were separated from the SVF, which contains blood vessels and preadipocytes (7,8). The SVF was plated to separate nonadherent blood vessels from preadipocytes, which attached to the dish. PLAP activity was seen in floating adipocytes and strongly in mural-like cells that lined vessels and that resemble adipocyte precursors in their location, appearance, and frequency (8). Upon brief culture of the adherent SVF fraction, small PLAP-positive colonies formed with a frequency and morphology similar to that of previously described adipocyte progenitors (Fig. 5*B*). Consistent with this, *Boc* was expressed in total WAT and the SVF but much less in mature adipocytes (Fig. 5*C*). As expected, *Pparγ* expression was detected at the highest levels in WAT and adipocytes, whereas the SVF expressed lower levels (Fig. 5*C*). These data suggest that *Boc* is expressed in adipocyte progenitors.

BOC expression was next analyzed by Western blotting during differentiation of 3T3-L1 preadipocytes. BOC levels were relatively low during growth conditions and strongly induced when cells reached confluence, just prior to switching cultures to adipogenic induction medium (Fig. 6*A*). BOC levels were partially diminished when the cells were induced to differentiate, prior even to expression of the adipogenic regulators PPARγ and C/EBPα, but were restored to their peak during the later stages of differentiation (Fig. 6*A*). GAS1, another SHH coreceptor, was expressed with a pattern similar to that of BOC, although the effect of cell confluence was not observed (Fig. 6*A*). In contrast to BOC and GAS1, the BOC paralog CDO was barely detected in 3T3-L1 cells. CDO was expressed robustly by C2C12 myoblasts, whereas BOC levels were low in this cell line, relative to 3T3-L1 cells (Fig. 6*A*).

To investigate BOC's role in adipogenesis, we isolated MEFs from E13.5 $Boc^{+/+}$ and $Boc^{-/-}$ embryos and cultured them in adipogenic induction medium for 15 days (D15). $Boc^{-/-}$ MEFs had more Oil Red O–positive colonies at D15 than did $Boc^{+/+}$ MEFs (Fig. 6*B* and *C*). The timing of induction of lipogenic genes was similar between $Boc^{+/+}$ and $Boc^{-/-}$ MEFs, but expression of each was higher in the $Boc^{-/-}$ MEFs, as analyzed by semiquantitative RT-PCR (Fig. 6*D*). Additionally, levels of aP2, FAS, and C/EBPα proteins were elevated in $Boc^{-/-}$ MEFs at D3 and D6, relative to control MEFs (Fig. 6*E*). Therefore, similar to results in $Boc^{-/-}$ mice, *Boc* deficiency resulted in enhanced adipogenesis of MEFs in vitro.

SHH signaling suppresses adipogenesis, and BOC promotes SHH signaling as a coreceptor (16,18,20). The effects

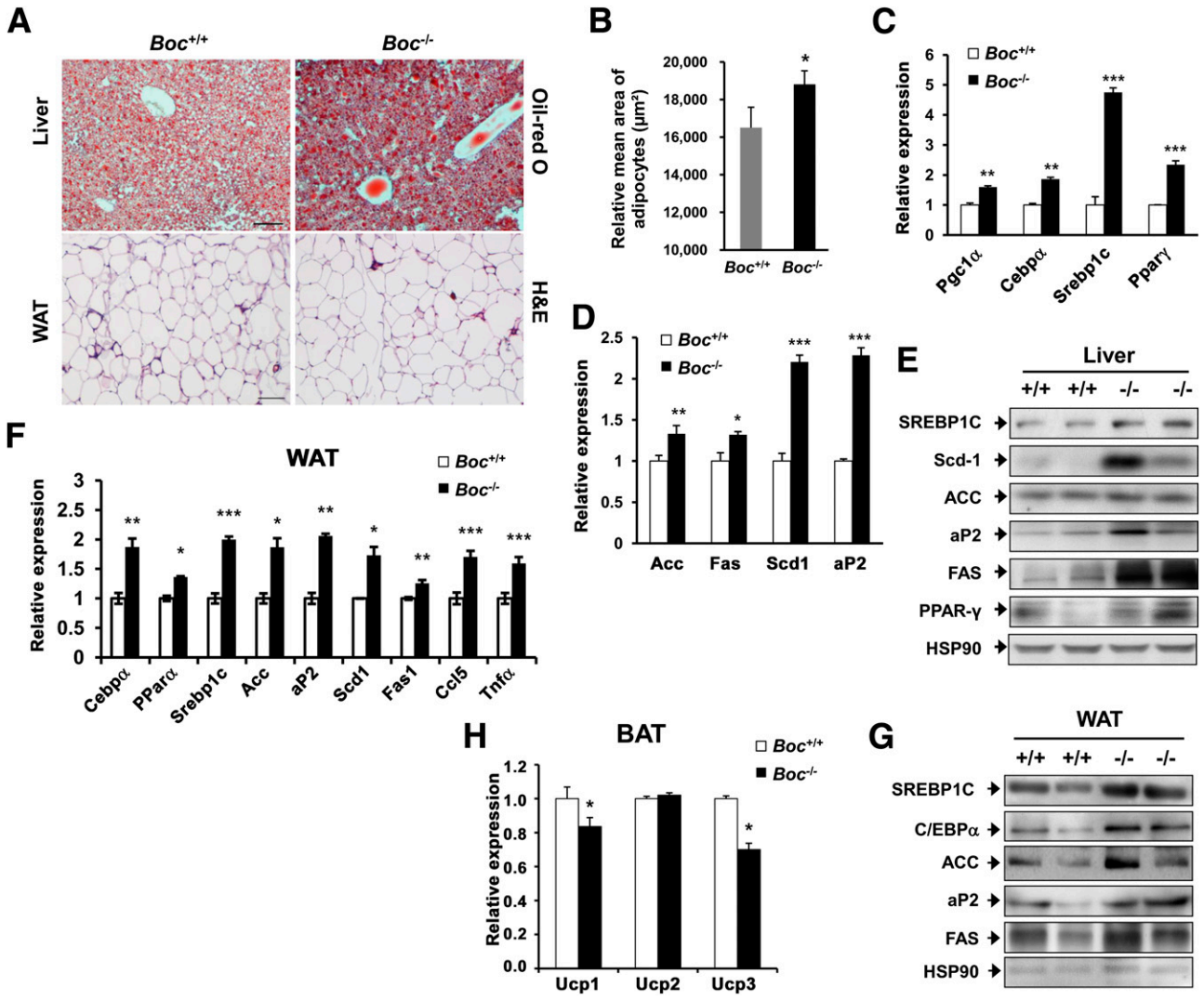

Figure 4—Exacerbated liver and WAT phenotypes in *Boc*$^{-/-}$ mice on HFD. *A*: Oil Red O–stained liver sections and H-E–stained WAT sections from *Boc*$^{+/+}$ and *Boc*$^{-/-}$ mice on HFD. Bar, 50 μm. *B*: Average area of adipocytes from sections of adult WAT from *Boc*$^{+/+}$ and *Boc*$^{-/-}$ mice. Values are means ± SD; $n = 3$. *$P < 0.05$. *C*: qRT-PCR analysis of expression of lipid metabolism genes in livers of *Boc*$^{+/+}$ and *Boc*$^{-/-}$ mice on HFD. Values are means of relative expression levels ± SD; $n = 3$. ***$P < 0.001$; **$P < 0.005$. *D*: qRT-PCR analysis of expression of adipogenic genes in livers of *Boc*$^{+/+}$ and *Boc*$^{-/-}$ mice on HFD. Values are means of relative expression levels ± SD; $n = 3$. ***$P < 0.001$; **$P < 0.005$; *$P < 0.05$. *E*: Western blot analysis of expression of lipid metabolism and adipogenic gene in livers of *Boc*$^{+/+}$ and *Boc*$^{-/-}$ mice on HFD. *F*: qRT-PCR analysis of expression of adipogenic, lipid metabolism, and adipokine genes in WAT of *Boc*$^{+/+}$ and *Boc*$^{-/-}$ mice on HFD. Values are means of relative expression levels ± SD; $n = 3$. ***$P < 0.001$; **$P < 0.005$; *$P < 0.05$. *G*: Western blot analysis of expression of lipid metabolism and adipogenic genes in WAT of *Boc*$^{+/+}$ and *Boc*$^{-/-}$ mice on HFD. *H*: qRT-PCR analysis of expression of uncoupling proteins in BAT of *Boc*$^{+/+}$ and *Boc*$^{-/-}$ mice on HFD. Values are means of relative expression levels ± SD; $n = 3$. *$P < 0.05$.

of BOC deficiency on adipogenesis may therefore be related to effects on SHH signaling. We initially addressed this question by analyzing adult *Boc*$^{+/+}$ and *Boc*$^{-/-}$ WAT for mRNA levels of various SHH signaling components by qRT-PCR. We examined expression of *Cdo*, *Gas1*, *Ptch1*, and *Gli1*; these genes not only encode components of the SHH pathway but their expression is also regulated by SHH pathway activity (*Ptch1* and *Gli1* expression is induced; expression of *Cdo* and *Gas1* is repressed, at least in early mouse embryos [11,18]). Expression of *Cdo*, *Gas1*, and *Ptch1* was significantly lower in *Boc*$^{-/-}$ WAT, compared with the *Boc*$^{-/-}$ WAT, whereas *Gli1* expression was similar (Fig. 7*A*). These results do not immediately suggest a major alteration of SHH signaling in *Boc*$^{-/-}$ WAT, but it may be simplistic to assume that expression of these genes is only regulated by SHH activity in a complex tissue that is also perturbed by loss of BOC.

To address this question further, expression of these genes in *Boc*$^{+/+}$ and *Boc*$^{-/-}$ MEFs during adipogenic differentiation was analyzed by semiquantitative RT-PCR. Expression of *Gli1*, *Ptch1*, and *Boc* was enhanced at day 2 of adipogenic differentiation in *Boc*$^{+/+}$ cells (Fig. 7*B*).

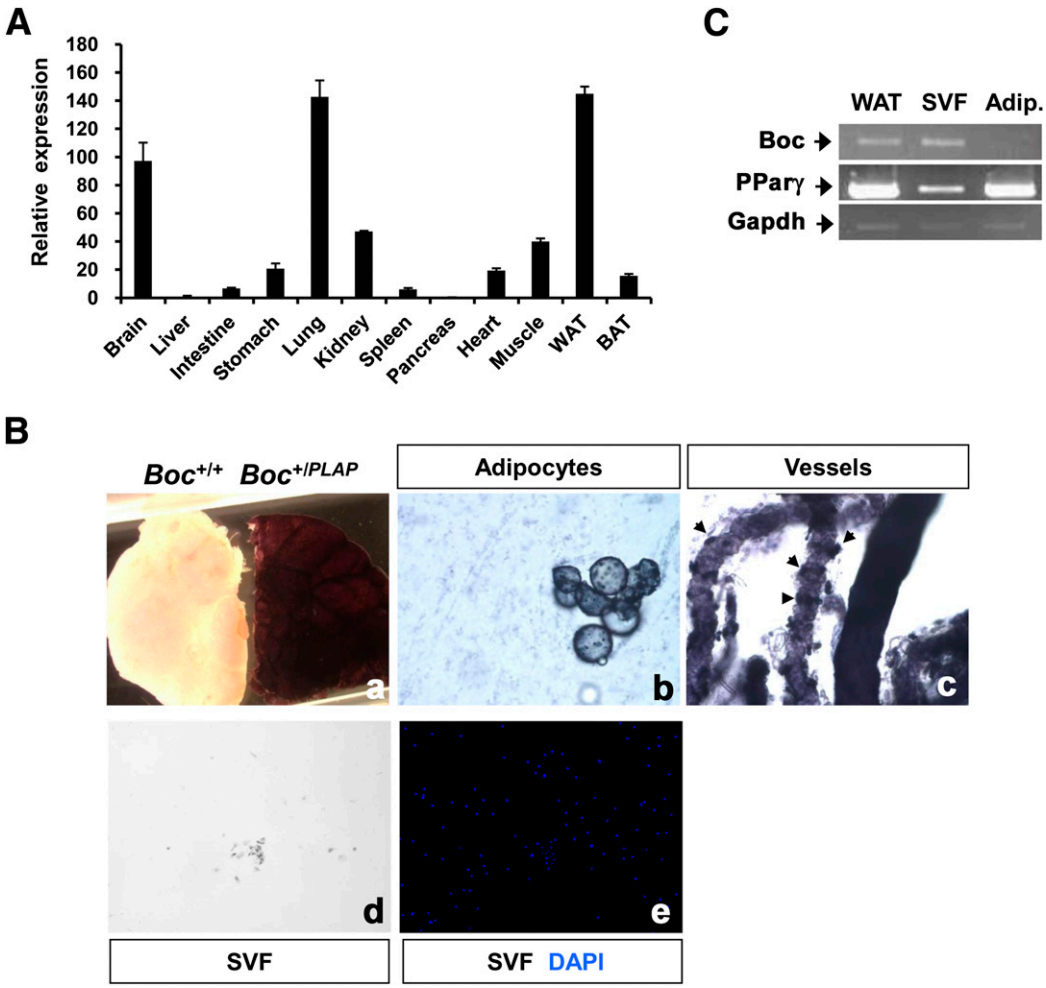

Figure 5—Analysis of *Boc* expression. *A*: qRT-PCR analysis of *Boc* expression in various adult tissues. Values are means of relative expression levels ± SD; $n = 3$. *L32* expression is set as 1. *B*: Alkaline phosphatase staining of WAT from $Boc^{+/+}$ and $Boc^{+/-}$ mice (note the Boc^{-} allele drives expression of a PLAP reporter gene, designated here Boc^{PLAP}; see text) (*a*). Alkaline phosphatase staining of isolated WAT adipocytes from $Boc^{+/PLAP}$ mice (*b*). Alkaline phosphatase staining of isolated vessels from the SVF from WAT of $Boc^{+/PLAP}$ mice, and stromal cells are marked by arrows (*c*). Alkaline phosphatase staining of adherent cells from the SVF from WAT of $Boc^{+/PLAP}$ mice (*d*). DAPI staining of the same culture shown in *d* (*e*). *C*: Semiquantitative RT-PCR analysis of *Boc* and *Pparγ* expression in WAT, SVF, and adipocytes (Adip.). *Gapdh* served as a loading control.

Induction of *Gli1* and *Ptch1* was diminished in $Boc^{-/-}$ MEFs and remained lower than in control cells throughout the differentiation time course (Fig. 7*B*). Western blot analyses revealed a similar pattern for GLI1 and PTCH1 protein levels (Fig. 7*C*). As *Gli1* and *Ptch1* are both direct SHH pathway target genes, these data suggest that BOC deficiency impairs SHH signaling activation during adipogenesis. Interestingly, *Cdo* was not expressed in $Boc^{+/+}$ cells but was abnormally induced in $Boc^{-/-}$ MEFs at D6 (Fig. 7*B*); however, CDO protein levels were too low for detection by Western blot (not shown). *Gas1* expression was not altered through the adipogenic differentiation time course and was similar in $Boc^{+/+}$ and $Boc^{-/-}$ MEFs (Fig. 7*B* and *C*).

BOC's major function in SHH signaling is as a coreceptor with PTCH1 (16). It would therefore be predicted that $Boc^{-/-}$ MEFs would remain sensitive to inhibition of adipogenic differentiation by activation of the SHH pathway at a point downstream of ligand reception. To test this notion, $Boc^{+/+}$ and $Boc^{-/-}$ MEFs were induced to differentiate in the presence of the SMO agonist purmorphamine, followed by Oil Red O staining at D12. Purmorphamine treatment resulted in strong reduction of adipocyte differentiation in both $Boc^{+/+}$ and $Boc^{-/-}$ MEFs (Fig. 7*D* and *E*). Expression of *aP2*, *Fas*, and *Scd1* was also analyzed in purmorphamine-treated $Boc^{+/+}$ and $Boc^{-/-}$ MEFs at D6 by qRT-PCR. In agreement with the Oil Red O staining results in Fig. 7*C* and *D*, *aP2*, *Fas*, and *Scd1* expression was higher in vehicle-treated $Boc^{-/-}$ MEFs than vehicle-treated $Boc^{+/+}$ MEFs but was decreased by purmorphamine treatment in both $Boc^{+/+}$ and $Boc^{-/-}$ MEFs (Fig. 7*F*). Western blot analyses revealed a similar pattern of aP2, FAS, and C/EBPα protein levels (Fig. 7*G*). These data indicate that activation of HH signaling

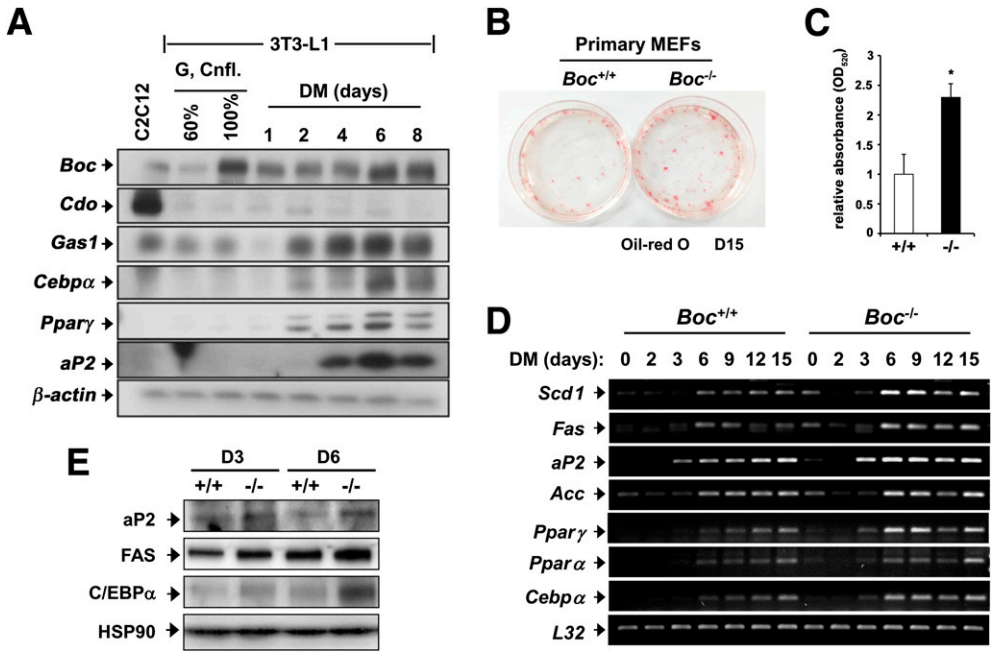

Figure 6—*Boc*$^{-/-}$ MEFs show enhanced adipogenesis. *A*: Western blot analysis of various proteins during a time course of adipogenic differentiation of 3T3-L1 cells. Lysates of 3T3-L1 cell cultures in growth medium (G) at 60 and 100% confluence (Cnfl.) or for the indicated number of days in differentiation medium (DM) were blotted with the indicated antibodies. β-Actin served as a loading control. *B*: Enhanced adipogenesis of *Boc*$^{-/-}$ MEFs relative to *Boc*$^{+/+}$ MEFs. Cultures were stained with Oil Red O after 15 days in differentiation medium. *C*: Quantification of Oil Red O staining by spectrophotometry at a wavelength of 520 nm relative to control sample. Values are means ± SD; $n = 3$. *$P < 0.05$. *D*: Semiquantitative RT-PCR analysis of expression of various genes induced during a time course of adipogenesis by *Boc*$^{+/+}$ and *Boc*$^{-/-}$ MEFs. *L32* served as a loading control. *E*: Western blot analysis of various adipogenic proteins in *Boc*$^{+/+}$ and *Boc*$^{-/-}$ MEFs at D3 and D6.

downstream of BOC coreceptor function is still sufficient to inhibit adipogenesis. BOC plays redundant roles with CDO and GAS1 as SHH coreceptors (13,16,19). Our findings here suggest that BOC plays a partially rate-limiting role in SHH signaling during adipogenic differentiation of MEFs. To assess whether *Boc*$^{-/-}$ MEFs were still responsive to the SHH ligand itself, *Boc*$^{+/+}$ and *Boc*$^{-/-}$ MEFs were induced to differentiate into adipocytes in the presence of exogenous, recombinant SHH for 12 days and analyzed by Oil Red O staining and qRT-PCR for adipogenic markers. Adipogenic differentiation of both *Boc*$^{+/+}$ and *Boc*$^{-/-}$ MEFs was inhibited to a similar degree (Fig. 7*H–J*). These results suggest that although loss of BOC may diminish endogenous SHH signaling during adipogenesis, expression of other coreceptors is likely sufficient to override the lack of BOC in *Boc*$^{-/-}$ MEFs and confer responsiveness to exogenous SHH.

DISCUSSION

Genetic factors that contribute to obesity-related WAT accumulation are poorly understood. The HH pathway plays a conserved role in adipogenesis, inhibiting fat formation (29–32). Mice with elevated HH signaling globally due to a hypomorphic *Ptch1* mutation, or in the adipocyte lineage via conditional targeted mutagenesis of *Sufu*, have sharply diminished WAT (33,34). Although these studies indicate that a genetic gain of function in HH pathway activity blocks adipogenesis, the converse has not been shown, i.e., that reduced HH pathway function results in WAT accumulation.

We report that mice lacking the HH coreceptor BOC displayed age-related overweight, with an increase in WAT, but not in the weight of internal organs. Furthermore, they had an exacerbated response to HFD, including enhanced weight gain and adipocyte hypertrophy, livers with greater fat accumulation, and elevated expression of genes related to adipogenesis, lipid metabolism, and adipokine production. *Boc*$^{-/-}$ MEFs showed enhanced adipogenesis and had reduced expression of the direct HH pathway target genes, *Gli1* and *Ptch1*, during adipogenic differentiation. Therefore, loss of BOC, and an associated decrease in HH signaling, in WAT precursor cells may underlie the age-related overweight and enhanced response to HFD seen in *Boc*$^{-/-}$ mice. Consistent with this possibility, *Boc* is prominently expressed in WAT, particularly in cells of the SVF that may function as adipocyte precursors. However, adipogenesis per se is not thought to be the prime driver of obesity (4,5), so it is not clear that moderate loss of HH function would be sufficient to override regulatory mechanisms of energy balance to drive enhanced adiposity. In fact, a role for loss of BOC outside the adipose lineage may be a major

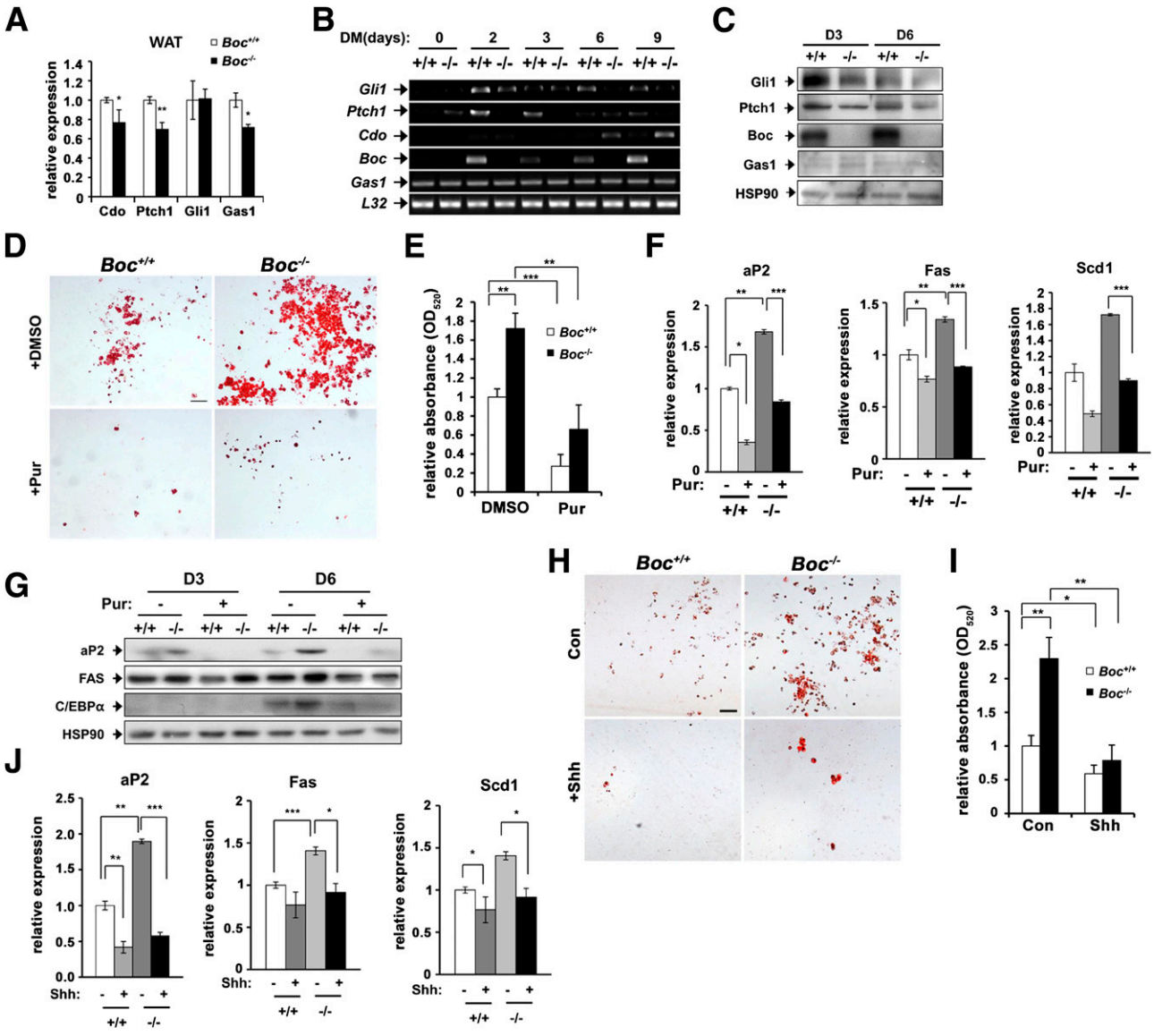

Figure 7—HH target gene expression is reduced in $Boc^{-/-}$ MEFs, and exogenous stimulation of HH pathway activity represses their adipogenic differentiation. *A*: qRT-PCR analysis of HH pathway component genes in WAT from $Boc^{+/+}$ and $Boc^{-/-}$ mice. Values are means of relative expression levels ± SD; $n = 3$. $^{**}P < 0.005$; $^{*}P < 0.05$. *B*: Semiquantitative RT-PCR analysis of HH pathway component genes during a time course of adipogenesis by $Boc^{+/+}$ (+/+) and $Boc^{-/-}$ (−/−) MEFs. *L32* served as a loading control. *C*: Western blot analysis of expression of HH pathway components in $Boc^{+/+}$ and $Boc^{-/-}$ MEFs at D3 and D6. *D*: The SMO agonist purmorphamine (Pur) inhibited adipogenic differentiation of both $Boc^{+/+}$ and $Boc^{-/-}$ MEFs. Cultures were stained with Oil Red O after 15 days in differentiation medium. *E*: Quantification of Oil Red O staining by spectrophotometry at a wavelength of 520 nm relative to the control sample. Values are means ± SD; $n = 3$. $^{**}P < 0.005$; $^{***}P < 0.001$. *F*: qRT-PCR analysis of expression of *aP2*, *Fas*, and *Scd1* in cultures of +/+ and −/− MEFs cultured in differentiation medium for 6 days plus or minus Pur. Values are means of relative expression levels ± SD; $n = 3$. $^{***}P < 0.001$; $^{**}P < 0.005$; $^{*}P < 0.05$. *G*: Western blot analysis of adipogenic proteins in cultures of +/+ and −/− MEFs cultured in differentiation medium for 3 or 6 days plus or minus Pur. *H*: SHH inhibited adipogenic differentiation of both $Boc^{+/+}$ and $Boc^{-/-}$ MEFs. Cultures were stained with Oil Red O after 15 days in differentiation medium. *I*: Quantification of Oil Red O staining by spectrophotometry at a wavelength of 520 nm relative to the control sample. Values are means ± SD; $n = 3$. $^{**}P < 0.005$; $^{*}P < 0.05$. *J*: qRT-PCR analysis of expression of *aP2*, *Fas*, and *Scd1* in cultures of +/+ and −/− MEFs cultured in differentiation medium for 6 days plus or minus SHH. Values are means of relative expression levels ± SD; $n = 3$. $^{***}P < 0.001$; $^{**}P < 0.005$; $^{*}P < 0.05$.

contributor to the enhanced adiposity of $Boc^{-/-}$ mice, as these animals had alterations in some metabolic parameters, including decreased body temperature and locomotive activity. *Boc* is expressed in the developing and adult central nervous system, albeit at low levels in the hypothalamus, a key structure for energy balance regulation (36). Construction of a *Boc* conditional mutant mouse line will be required to address this point. It is worth noting that the global *Ptch1* and adipose-specific *Sufu* mutants did not display substantial alterations in metabolic parameters or in the GTT (33,34); however, these animals had reduced WAT, rather than overweight or obesity.

The effects of *Boc* mutation are relatively modest. $Boc^{-/-}$ mice became overweight by 4 months of age but were not obese. They showed elevated levels of serum triglycerides and nonesterified fatty acids, and defects in GTT and ITT, when on the HFD, but their fasted blood glucose and insulin levels were similar to those of control mice. This may reflect redundancy of BOC with GAS1 and CDO, additional HH coreceptors. These coreceptors have overlapping functions and are collectively required for HH signaling in the mouse embryo (13,16,19). *Gas1* was expressed in 3T3-L1 cells and MEFs, whereas *Cdo* was expressed at low levels in these cells. Furthermore, *Cdo* mutant mice do not have an overweight phenotype (unpublished data). GAS1 may therefore function in the absence of BOC to provide a level of HH coreceptor activity that limits the effects of loss of BOC to overweight rather than full-blown obesity. As expected, activation of the HH pathway downstream of BOC with the SMO agonist purmorphamine inhibited adipogenesis of both $Boc^{+/+}$ and $Boc^{-/-}$ MEFs. However, adipogenesis of both cell types was also inhibited by recombinant SHH. We hypothesize that the presence of GAS1, and perhaps CDO, was sufficient to allow a strong response to exogenous SHH, but that loss of BOC was enough to cause a diminished response to endogenously produced HH ligand. It seems likely, therefore, that genetic removal of *Gas1*, and perhaps *Cdo*, from $Boc^{-/-}$ mice would result in further loss of HH coreceptor activity and worsen the overweight phenotype; this is what is seen in neural tube patterning (13). Testing this notion will also require a conditional mutagenesis approach, as double mutants for any of these three factors have severe phenotypes and are not viable (13,19).

Genetic variants in the HH pathway may play a role in WAT accumulation in human obesity. Loss-of-function mutations in human genes encoding several HH pathway components, including *CDO* and *GAS1*, are associated with holoprosencephaly, a common and often devastating developmental defect of the forebrain (15,37,38). Mice with mutations in these genes are good models for holoprosencephaly (39). However, $Boc^{-/-}$ mice do not have holoprosencephaly and are viable (19). Therefore, it is possible that "weak" *BOC* alleles may exist in the human population and contribute to WAT accumulation in individuals with additional genetic or lifestyle-based predisposition to obesity. It is interesting that the effects of *Boc* mutation were seen with age and diet, two variables involved with weight gain. Genome-wide association studies have not linked *BOC* to obesity, although that is not surprising given that $Boc^{-/-}$ mice are overweight, not obese. Many variant *BOC* alleles have been documented in the 1000 Genomes data, including many with likely deleterious changes. Some of these could act as modifier genes in individuals with obesity or metabolic disorders. In summary, the HH pathway is a conserved inhibitor of fat formation, and we report for the first time a loss-of-function mutation in the HH pathway associated with WAT accumulation and overweight.

Funding. This research was supported by National Institutes of Health grant AR-46207 (R.S.K.) and a National Research Foundation of Korea grant funded by the Korea Government (NRF-2011-0017315) (J.-S.K.).

Duality of Interest. No potential conflicts of interest relevant to this article were reported.

Author Contributions. H.-J.L., S.-B.J., A.I.R., H.-J.L., M.-J.K., and S.-H.K. contributed to the experimental design, research, data analysis, and review of the manuscript. R.S.K. and J.-S.K. contributed to experimental design, data analysis, and writing of the manuscript. R.S.K. and J.-S.K. are the guarantors of this work and, as such, had full access to all the data in the study and takes responsibility for the integrity of the data and the accuracy of the data analysis.

Prior Presentation. This work was presented as a poster at the International Conference of the Korean Society for Molecular and Cellular Biology, Seoul, Korea, 9–11 October 2013.

References

1. Blüher M. Adipose tissue dysfunction in obesity. Exp Clin Endocrinol Diabetes 2009;117:241–250
2. Ogden CL, Carroll MD, Kit BK, Flegal KM. Prevalence of childhood and adult obesity in the United States, 2011-2012. JAMA 2014;311:806–814
3. Berry R, Jeffery E, Rodeheffer MS. Weighing in on adipocyte precursors. Cell Metab 2014;19:8–20
4. Rosen ED, Spiegelman BM. What we talk about when we talk about fat. Cell 2014;156:20–44
5. Spiegelman BM, Flier JS. Obesity and the regulation of energy balance. Cell 2001;104:531–543
6. Rosen ED, MacDougald OA. Adipocyte differentiation from the inside out. Nat Rev Mol Cell Biol 2006;7:885–896
7. Rodeheffer MS, Birsoy K, Friedman JM. Identification of white adipocyte progenitor cells in vivo. Cell 2008;135:240–249
8. Tang W, Zeve D, Suh JM, et al. White fat progenitor cells reside in the adipose vasculature. Science 2008;322:583–586
9. McMahon AP, Ingham PW, Tabin CJ. Developmental roles and clinical significance of hedgehog signaling. Curr Top Dev Biol 2003;53:1–114
10. Briscoe J, Thérond PP. The mechanisms of Hedgehog signalling and its roles in development and disease. Nat Rev Mol Cell Biol 2013;14:416–429
11. Jiang J, Hui CC. Hedgehog signaling in development and cancer. Dev Cell 2008;15:801–812
12. Varjosalo M, Taipale J. Hedgehog: functions and mechanisms. Genes Dev 2008;22:2454–2472
13. Allen BL, Song JY, Izzi L, et al. Overlapping roles and collective requirement for the coreceptors GAS1, CDO, and BOC in SHH pathway function. Dev Cell 2011;20:775–787
14. Allen BL, Tenzen T, McMahon AP. The Hedgehog-binding proteins Gas1 and Cdo cooperate to positively regulate Shh signaling during mouse development. Genes Dev 2007;21:1244–1257
15. Bae GU, Domené S, Roessler E, et al. Mutations in CDON, encoding a hedgehog receptor, result in holoprosencephaly and defective interactions with other hedgehog receptors. Am J Hum Genet 2011;89:231–240
16. Izzi L, Lévesque M, Morin S, et al. Boc and Gas1 each form distinct Shh receptor complexes with Ptch1 and are required for Shh-mediated cell proliferation. Dev Cell 2011;20:788–801
17. Martinelli DC, Fan CM. Gas1 extends the range of Hedgehog action by facilitating its signaling. Genes Dev 2007;21:1231–1243
18. Tenzen T, Allen BL, Cole F, Kang JS, Krauss RS, McMahon AP. The cell surface membrane proteins Cdo and Boc are components and targets of the Hedgehog signaling pathway and feedback network in mice. Dev Cell 2006;10:647–656

19. Zhang W, Hong M, Bae G-U, Kang JS, Krauss RS. *Boc* modifies the holoprosencephaly spectrum of *Cdo* mutant mice. Dis Model Mech 2011;4:368–380
20. Zhang W, Kang J-S, Cole F, Yi MJ, Krauss RS. Cdo functions at multiple points in the Sonic Hedgehog pathway, and Cdo-deficient mice accurately model human holoprosencephaly. Dev Cell 2006;10:657–665
21. Kang J-S, Gao M, Feinleib JL, Cotter PD, Guadagno SN, Krauss RS. CDO: an oncogene-, serum-, and anchorage-regulated member of the Ig/fibronectin type III repeat family. J Cell Biol 1997;138:203–213
22. Kang J-S, Mulieri PJ, Hu Y, Taliana L, Krauss RS. BOC, an Ig superfamily member, associates with CDO to positively regulate myogenic differentiation. EMBO J 2002;21:114–124
23. Martinelli DC, Fan C-M. The role of Gas1 in embryonic development and its implications for human disease. Cell Cycle 2007;6:2650–2655
24. Zheng X, Mann RK, Sever N, Beachy PA. Genetic and biochemical definition of the Hedgehog receptor. Genes Dev 2010;24:57–71
25. Fabre PJ, Shimogori T, Charron F. Segregation of ipsilateral retinal ganglion cell axons at the optic chiasm requires the Shh receptor Boc. J Neurosci 2010;30:266–275
26. Harwell CC, Parker PR, Gee SM, et al. Sonic hedgehog expression in corticofugal projection neurons directs cortical microcircuit formation. Neuron 2012;73:1116–1126
27. Okada A, Charron F, Morin S, et al. Boc is a receptor for sonic hedgehog in the guidance of commissural axons. Nature 2006;444:369–373
28. Sánchez-Arrones L, Nieto-Lopez F, Sánchez-Camacho C, et al. Shh/Boc signaling is required for sustained generation of ipsilateral projecting ganglion cells in the mouse retina. J Neurosci 2013;33:8596–8607
29. Fontaine C, Cousin W, Plaisant M, Dani C, Peraldi P. Hedgehog signaling alters adipocyte maturation of human mesenchymal stem cells. Stem Cells 2008; 26:1037–1046
30. Spinella-Jaegle S, Rawadi G, Kawai S, et al. Sonic hedgehog increases the commitment of pluripotent mesenchymal cells into the osteoblastic lineage and abolishes adipocytic differentiation. J Cell Sci 2001;114:2085–2094
31. Suh JM, Gao X, McKay J, McKay R, Salo Z, Graff JM. Hedgehog signaling plays a conserved role in inhibiting fat formation. Cell Metab 2006;3: 25–34
32. Xu Z, Yu S, Hsu CH, Eguchi J, Rosen ED. The orphan nuclear receptor chicken ovalbumin upstream promoter-transcription factor II is a critical regulator of adipogenesis. Proc Natl Acad Sci U S A 2008;105:2421–2426
33. Li Z, Zhang H, Denhard LA, Liu LH, Zhou H, Lan ZJ. Reduced white fat mass in adult mice bearing a truncated Patched 1. Int J Biol Sci 2008;4: 29–36
34. Pospisilik JA, Schramek D, Schnidar H, et al. *Drosophila* genome-wide obesity screen reveals hedgehog as a determinant of brown versus white adipose cell fate. Cell 2010;140:148–160
35. Sun H, Taneja R. Analysis of transformation and tumorigenicity using mouse embryonic fibroblast cells. Methods Mol Biol 2007;383:303–310
36. Mulieri PJ, Kang J-S, Sassoon DA, Krauss RS. Expression of the *boc* gene during murine embryogenesis. Dev Dyn 2002;223:379–388
37. Pineda-Alvarez DE, Roessler E, Hu P, et al. Missense substitutions in the GAS1 protein present in holoprosencephaly patients reduce the affinity for its ligand, SHH. Hum Genet 2012;131:301–310
38. Roessler E, Muenke M. The molecular genetics of holoprosencephaly. Am J Med Genet C Semin Med Genet 2010;154C:52–61
39. Schachter KA, Krauss RS. Murine models of holoprosencephaly. Curr Top Dev Biol 2008;84:139–170